# Time-periodic lattice of spiral pairs in excitable media

A. Rabinovitch,[1,*] Y. Biton,[1] D. Braunstein,[2] M. Friedman,[3] and I. Aviram[1]
[1]*Physics Department, Ben-Gurion University of the Negev, Beer-Sheva, 84105, Israel*
[2]*Physics Department Shamoon College of Engineering, Beer-Sheva, Israel*
[3]*Department of Information Systems Engineering, Ben-Gurion University, Beer Sheva 84105, Israel*
(Received 20 June 2011; revised manuscript received 8 September 2011; published 30 March 2012)

The feasibility of a spiral-type solution, periodic both in time and in space, of a reaction-diffusion equation (specifically the FitzHugh-Nagumo system) in an excitable medium is numerically demonstrated. The solution consists of arrays of interacting spiral pairs, which repeatedly create by partial annihilation a system of residual portions (RPs). The latter behaves as a source to the next generation of the spiral-pair array. If basic (highest) translational symmetry is not conserved, pointwise perturbations, above a certain threshold, are shown to be able to destroy the pattern after a certain transient time by changing its symmetry. If the basic translational symmetry is preserved, such perturbations do not cause destruction unless occurring at the nearest vicinity of the RP site. Singular value decomposition methods are used to analyze the structure of the pattern, revealing the importance of the spiral pairs and the RPs.

DOI: 10.1103/PhysRevE.85.036217 PACS number(s): 89.75.Kd, 87.19.Hh, 87.10.−e

## I. INTRODUCTION

Periodic spatial patterns (lattices) and periodic temporal patterns (oscillators) have been intensively studied hitherto. Periodic spatiotemporal patterns (PSTPs) (i.e., patterns that are periodic both in time and in space) are usually classified as waves, either standing or propagating. Two-dimensional (2D) waves were investigated mainly as waves on fluid surfaces (see, e.g., Ref. [1]). PSTPs of the convective fields appear in the Rayleigh-Benard analysis [2]. Spiral-type PSTPs have been observed experimentally in different physical and biological instances. Atrial fibrillation is the most abundant cardiac arrhythmia [3]. Though not fatal in itself, it can lead to complications (clots), which are life threatening. Recent studies [4,5] by optical mapping of animals' hearts exhibit periodic spatial patterns that are also repeated in time. Some PSTPs appear in the brain [6,7] and can perhaps be connected with the memory process. Note that in Ref. [6] the spatial phases are only randomly chosen and that our periodic spatial patterns can lead to both sequences and songs in the language of Ref. [7]. Recurrent dreams or memories may possibly be obtained from PSTPs in the nervous system under special conditions.

In this work we demonstrate the feasibility of a spiral-pair PSTP solution to a nonlinear system [the FitzHugh-Nagumo (FHN)] in a 2D excitable medium. The FHN system and the patterns emerging from it have been extensively analyzed since the 1970s (see, e.g., Refs. [8–10] and a recent review of the use of FHN for neurodynamics [11]). Thus, repetitive activity in the FHN is discussed in Ref. [8], while the existence of temporal orbits and pulse waves are respectively treated in Refs. [9] and [10]. The possibility of a single temporally periodic spiral-pair solution to the system is also well known [12,13]; however, a description of a spiral-type solution in an excitable medium that is also periodic in space is needed. A single spiral pair is usually created by the vulnerable window technique devised by Winfree [14,15]. We use here our unidirectional method [16,17] for the creation of the spiral pairs. In this method, two adjacent squares of different sizes are simultaneously stimulated in an excitable medium. Two short current surges are induced at time zero: the larger square is activated below the threshold, while the smaller one, above the threshold. This kind of forcing leads to unidirectional spiral pair pulse propagation [18]. Spiraling inwards, the arms of the pair collide with each other and are annihilated. Under appropriate conditions [16], a small residual portion (RP) of the colliding arms outlasts the collision, and becomes the source of new spiral pairs. Here we use this method to generate spiral pair PSTPs. The parameter ranges of this solution are calculated and the possible generation process is investigated.

## II. MODEL

We use the 2D FitzHugh Nagumo system [12] to characterize the medium, and solve it in a square domain. It reads:

$$\frac{\partial v}{\partial t}=D\left(\frac{\partial^2}{\partial x^2}+\frac{\partial^2}{\partial y^2}\right)v+v(v-a)(1-v)-w+\delta(t)I(x,y),$$
$$\frac{\partial w}{\partial t}=\varepsilon(v-dw), \qquad (1)$$

where all variables are dimensionless. For the heart tissue, $v$ is the action-potential, $w$ is the refractivity, an inhibitory variable, and $\delta(t)I(x,y)$ is the instantaneous input current. The constants $D$, $a$, and $\varepsilon$ are the diffusion constant, the excitability parameter, and the ratio between the fast and the slow time constants, respectively. The constant $d$ controls the shape of the wave. $\delta(t)$ is the Dirac delta function and $I(x,y)$ is the spatial shape of the amplitude of the applied current. The FHN equations are solved in a square domain of 80 × 80 grid points (a unit cell) with periodic boundary conditions. This unit cell comprises four squares 40 × 40 each and the initial current is applied to the two diagonal squares [see Fig. 1(a)]. The results here are shown in a larger domain of 160 × 160 (4 unit cells) for the sake of clarity of presentation. All calculations were carried out with the parameter values $a=0.12, D=0.2, \varepsilon=0.005, d=3$, unless

*avinoam@bgu.ac.il

 

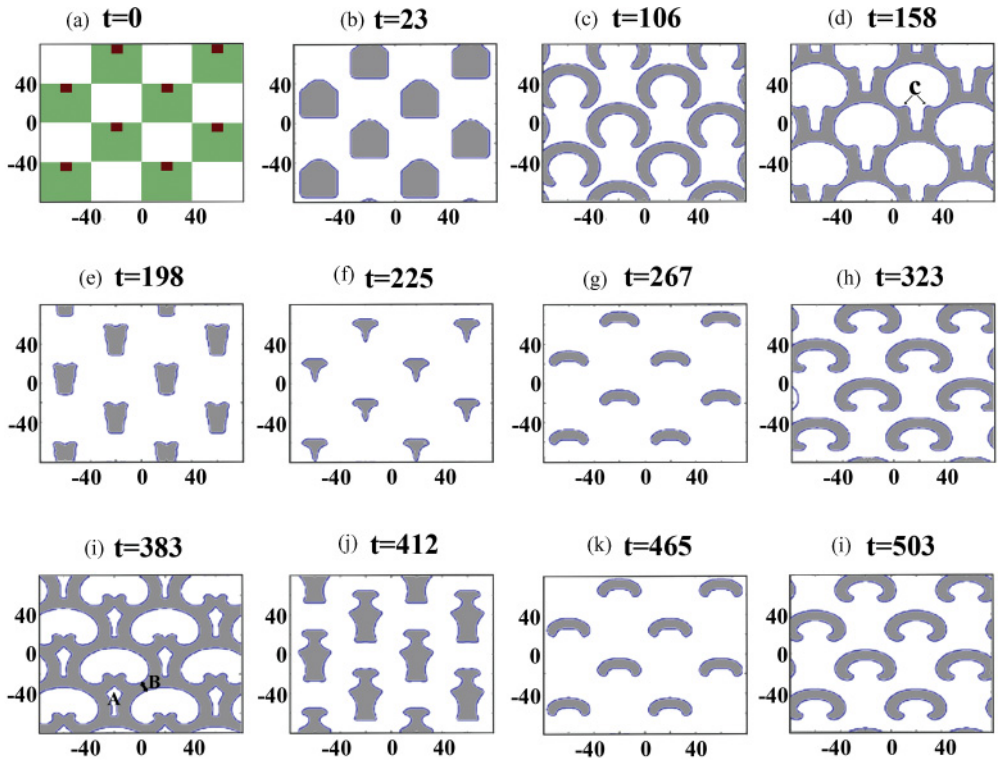


FIG. 1. (Color online) Time evolution of $v(x, y)$ for the PSTP. Green large squares [appears as shaded area in part (a)] initially stimulated by a below-threshold pulse. Brown small squares [appears as darker areas in part (a)] initially stimulated by an above-threshold pulse. Gray shaded areas correspond to $v > 0.5$.

specified otherwise. The system of equations was solved by using for the time coordinate the second-order Euler forward finite difference, usually a stable scheme, often referred to as the second-order Runge-Kutta (RK2) method. The second-order derivatives in the spatial coordinates $x$ and $y$ were replaced by central differences. The time and space increments were $\Delta t = 0.125, \Delta x = \Delta y = 0.5$. This mesh provided sufficient accuracy, since a finer one ($\Delta t = 0.05, \Delta x = \Delta y = 0.25$) yielded no apparent change in the numerical solutions.

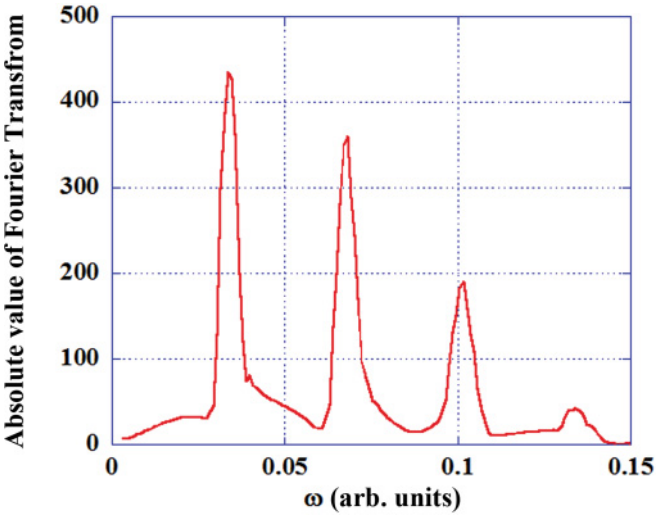


FIG. 2. (Color online) Absolute value of the Fourier transform of $v$ at $x = y = 0$; the dominant peak is at $\omega = 0.0335$.

## III. RESULTS

The initial input current $I(x,y)$ is applied to the pattern displayed in Fig. 1(a). There are two diagonal squares of size $40 \times 40$ (marked in green) in each unit cell of size $80 \times 80$ with periodic boundary conditions, in which the initial stimulation current amplitude is $A_1 = 0.1555$, just below the threshold value of 0.1556. The initial above-threshold stimulation, $A_2 = 0.2$, is applied in the smaller square of $8 \times 8$ (marked in brown), located adjacent to the upper side of the green square. No input current is applied to the white squares. For a system of four unit cells occupying a region of size $160 \times 160$, with periodic boundary conditions on the expanded perimeter, the dynamical evolution appeared to be identical to the computation of a unit cell ($80 \times 80$). Figure 1 illustrates the stages of the PSTP evolution for a lattice of 4 unit cells in order to emphasize the emerging patterns. Marked in gray are the areas where the value of $v$ is above 0.5 (videos are available [19]).

TABLE I. Parameter ranges for a single spiral pair (SSP) and for the lattice PSTP creation. Each parameter is varied while the others are kept constant at their respective mean values.

| Range Value (SSP) | Range Value (PSTP) | Parameter |
|---|---|---|
| $0.1 \leqslant D \leqslant 0.38$ | $0.1 \leqslant D \leqslant 0.35$ | $D$ |
| $0 < d \leqslant 3.4$ | $1 \leqslant d \leqslant 3.2$ | $d$ |
| $0.00496 \leqslant \varepsilon \leqslant 0.00540$ | $0.00496 \leqslant \varepsilon \leqslant 0.00540$ | $\varepsilon$ |
| $0.1197 \leqslant a \leqslant 0.1202$ | $0.1197 \leqslant a \leqslant 0.1202$ | $a$ |

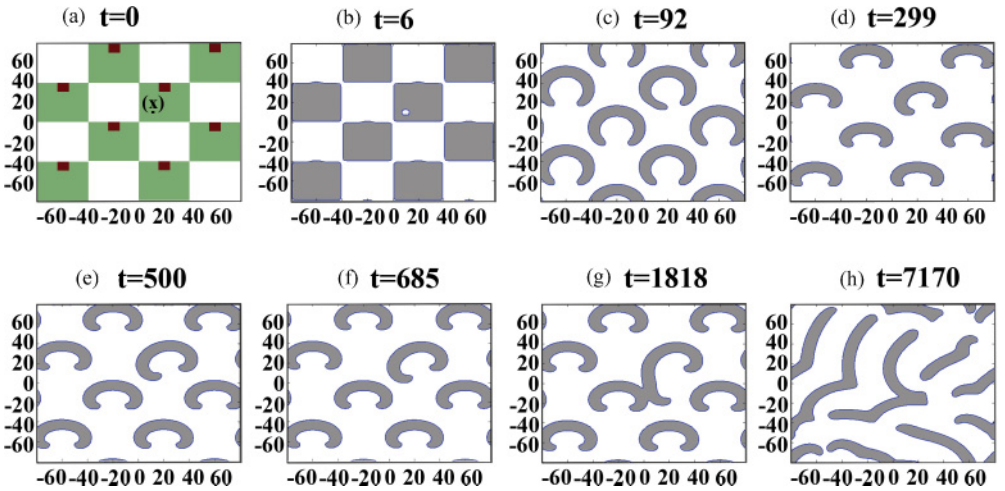


FIG. 3. (Color online) The effect of a point perturbation [marked by x in Fig. 3(a)] breaking the highest translational symmetry (in a $2 \times 2$ unit cell with periodic boundary conditions on the perimeter). The perturbation is located at $x = 10$, $y = 10$ and is applied at $t = 0$, intensity $I = 0.06$.

As can be seen, similar to the single spiral pair case, the patterns are based on a residual portion (RP), which remains unimpaired following an encounter of the arms of the structures and their partial annihilation. However, in contrast to the single case where the encounter is between the arms of the single spiral pair, the situation here is more complex. The encounter here occurs [Fig. 1(c)] between all diagonally nearest-neighbor spiral pairs, essentially between every foursome, creating first a lattice of colliding spiral pairs stretching across the entire lattice area [Figs. 1(d) and 1(i)]. This lattice then transforms into separate units [Fig. 1(e)] by two annihilation processes: being too small to survive, the holes, marked A in Fig. 1(i), disappear and the thin connecting bridges, B in Fig. 1(i), are gradually cut off. The units evolve into composite shapes [Fig. 1(j)] presenting a lower fuller part and an upper thinner part. The fuller part shrinks and disappears while the narrow one survives [Fig. 1(f)], and comprises the RP, which is the source of the next generation PSTP. The system was run for hundreds of periods and, following a transient time, an almost exact limit cycle is settled down asymptotically. Temporal Fourier spectra were computed at the following space coordinates: [(0, 0); (10, 10); (50, 0); (20, 50)], all producing almost identical results. One such spectrum is shown in Fig. 2. It is seen that the period is $T = 2\pi/w = 187.5$ time units, somewhat surprisingly equal to that for a single spiral pair in the unidirectional method [16,17] with the same set of parameter values. By a careful observation of the patterns, this equality of period can be explained as follows. For a single spiral pair, the arms of the pair must encounter each other (an autocollision) in order to create the RP. Here, although the arms of different spiral pairs meet and partly annihilate [intercollision, Fig. 1(c)], the actual RP is again created by an autocollision of the remaining tips [C in Fig. 1(d)] of each of the individual pairs. The intercollisions do, however, decrease the viability of the arms, making it harder to obtain the next RP (see below).

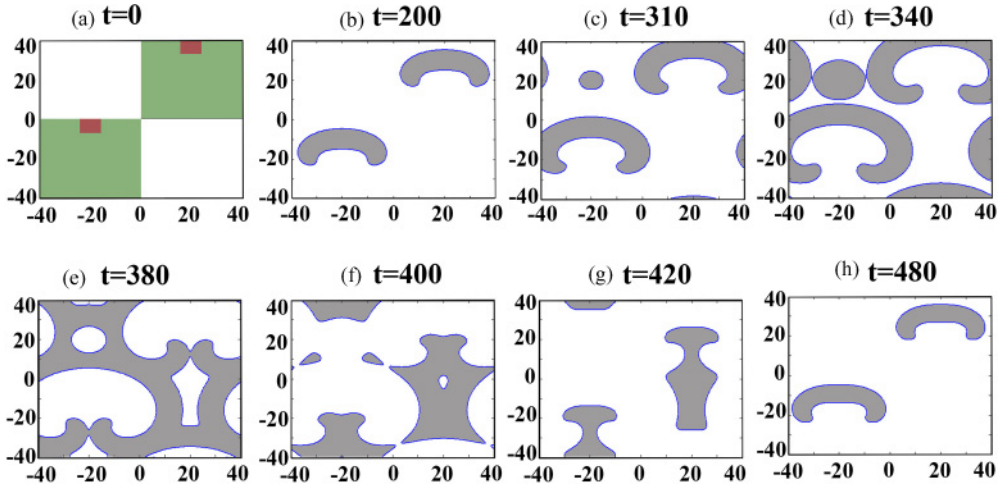


FIG. 4. (Color online) The influence of perturbation at ($x = -20$, $y = 20$, $t = 300$) in a single unit cell with periodic boundary conditions, which therefore implies that the same perturbation appears in every unit cell (highest translational symmetry conserved). $I = 0.2$, $\Delta L = 2 \times 2$, ($D = 0.2$, $a = 0.12$, $\varepsilon = 0.005$). Perturbation is at a distance from an RP.

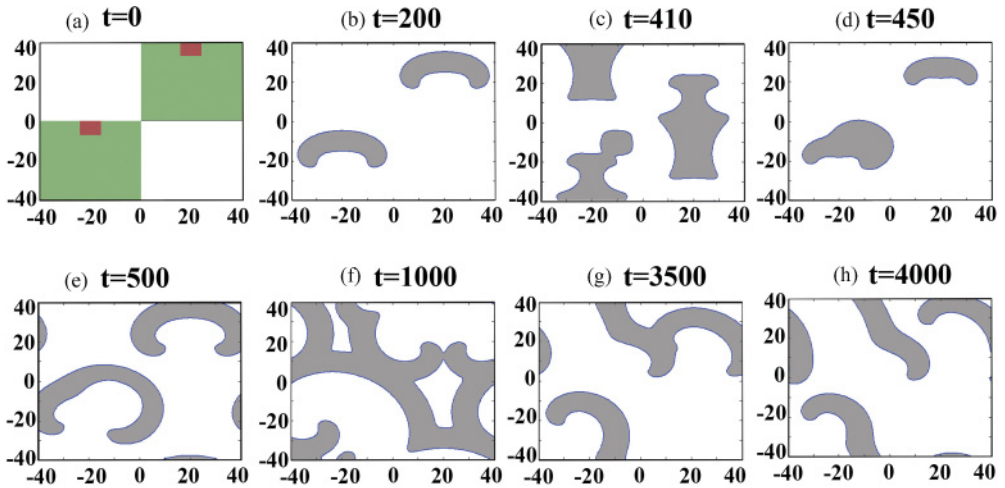


FIG. 5. (Color online) The influence of perturbation at ($x = -10$, $y = 10$, $t = 400$) in a single unit cell with periodic boundary conditions. $I = 0.2$, $\Delta L = 2 \times 2$, ($D = 0.2$, $a = 0.12$, $\varepsilon = 0.005$). Perturbation is near an RP.

The parameter ranges where the PSTP is present are given in Table I. They are compared to the ranges for a single spiral pair (SSP, no lattice). For both cases it is seen that while the ranges of $D$ and $d$ are quite large, the other two parameters can only stay within very narrow ranges. The restricting factor common to both cases is the ability to create a viable RP. It follows that the spiral arms collide not head-on but at their curved external parts [16]. The reduced ranges of $D$ and $d$ in the PSTP case are due to the interaction of each spiral pair with its neighbors [intercollisions, see, e.g., Fig. 1(d)]. For the ranges included in the SSP case but not in the PSTP this interaction diminishes somewhat the width of the spiral pair arms. The latter thus become weaker to such a degree that the RP resulting from their coalescence is no longer viable.

The transient period of the phenomenon is very short, lasting only until the first creation of the RP. Following this occurrence, absulute periodicity sets in.

## IV. STABILITY UNDER PERTURBATIONS

The PSTPs are quite delicate entities. In the seminal works [20–22] the stability of regular spirals produced by the complex Ginzburg-Landau equation was established, both as solutions to differential equations [20], and under perturbations by mutual interaction. Spiral stability encountering plane waves [23] is also to be noted. Due to their complex nature, the stability of the structures considered here is even more subtle. Not only must next generation RPs be created [16], but the intercollisions should be mild enough such that the retained arms strength should be sufficient for viable RPs. These severe conditions lead to a rather small stability range of the parameters (Table I). Moreover, even very small local perturbations, not conserving the system's translational symmetry, lead to structure disappearance, as is presently demonstrated.

A perturbation conserving the highest translational symmetry must be one that is periodically reproduced at the same location in every single unit cell, defined above. Such a perturbation will normally leave the dynamical pattern relatively stable. Alternatively, if the perturbation is applied, say, on every square cluster of four unit cells, the translational symmetry will be lowered (spatial period of two unit cell sides, in both directions), producing disordered patterns, and their ultimate destruction, as demonstrated in Fig. 3, above. The size of the studied system in Fig. 3 is ($160 \times 160$), comprising four unit cells, with periodic boundary conditions on its perimeter. The system is activated to produce unidirectional spiral pairs, as explained above. The perturbation consists of a weak ($I = 0.06$) instantaneous pulse, applied in a very small cluster of four grid points around the coordinates (10, 10). The time evolution of the perturbed system, from its seemingly innocuous appearance to a full disruption of the pattern, is clearly demonstrated. The perturbation first distorts its nearest

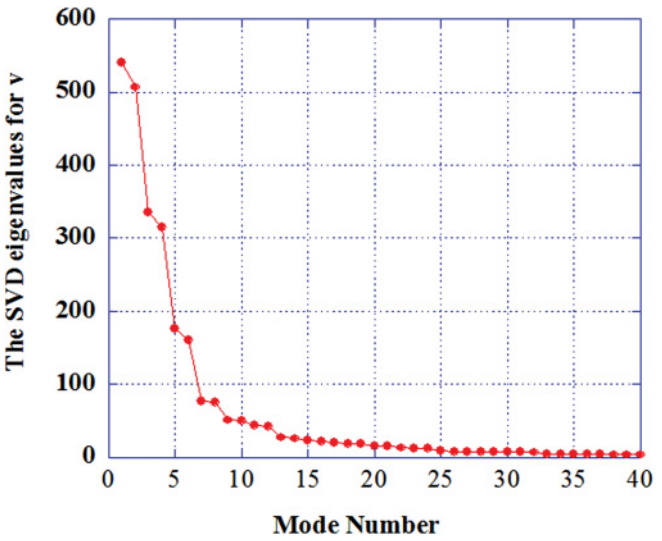


FIG. 6. (Color online) The SVD eigenvalues, $S$, for two complete periods of $v$.

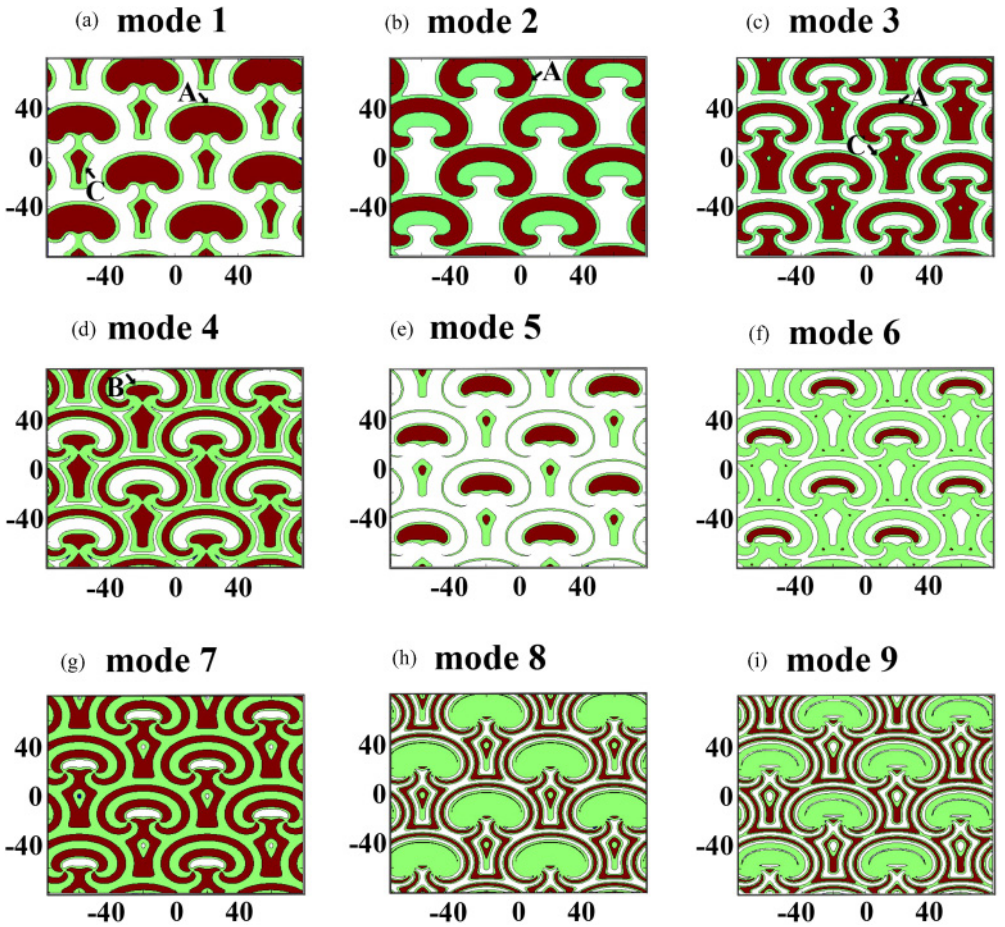


FIG. 7. (Color online) The leading SVD modes for $v$ ($t_1 = 240$, $t_2 = 618$, $\Delta t = 6$). Green (lightly shaded): $0 < v < 0.01$; Brown (darkly shaded): $0.01 < v < 0.5$.

spiral pair by slightly rotating it [Fig. 3(c)]. The rotated pair interacts with its nearest pairs which continue in this manner, and after a relatively long time, leads to a distorted pattern [Fig. 3(h)]. This pattern is not viable and ultimately completely disappears. The perturbation was applied at times, both within the transient period, and during the steady state of the PSTP, with no change in the destruction process. To demonstrate this point Fig. 3 depicts the situation where the perturbation is applied at the beginning of the process while Figs. 4 and 5 show the case where the perturbations are applied during the steady state.

Let us now examine a system in which the perturbations are applied periodically in every single unit cell, thus preserving the highest translational symmetry. It suffices to refer to a $(80 \times 80)$ square with periodic boundary conditions on the perimeter. It is observed that, unless applied in a close proximity of an RP, point perturbations, even large ones, do not cause any prolonged damage to the pattern. Figure 4 depicts the influence of a perturbation that is away from an RP while Fig. 5 shows the situation when it is close enough to one. It is seen that in the first case the system recovers from the perturbation and regains the original pattern, while in the latter case the pattern becomes chaotic after a relatively long period of time.

## V. STRUCTURE ANALYSIS BY SINGULAR VALUE DECOMPOSITION

In order to better understand the structure of the PSTPs, they were analyzed by the singular value decomposition (SVD) method. This method, also called proper orthogonal decomposition or the Karhunen-Loeve decomposition [24,25], is a technique to extract the dominant spatial (time-average) modes of a PSTP evolution. It generates a spatial vector basis arranged in order of seniority, such that the projection of the phenomenon onto these vectors in a sequential way yields, at each step, the best approximation to it, in a least square error sense.

The analysis is based on the method of snapshots [26]. The solution at each time point $t_i$, $i = 1,M$, is considered to be a snapshot made up of a fixed number of pixels, $x_k,k = 1,L$. The snapshot is converted into a vector $u(x,t_i)$ of values each depicting the action-potential amplitude at its specific pixel. All vectors thus constructed for all $t_i$ are assembled into a rectangular matrix $B$. The SVD method is applied to this matrix and leads to its left and right diagonalization: $USV^{\dagger} = B$, where $S$ contains the singular values (eigenvalues) on its diagonal. These values, arranged in a decreasing order, convey the sequence of energies (the order of importance) of

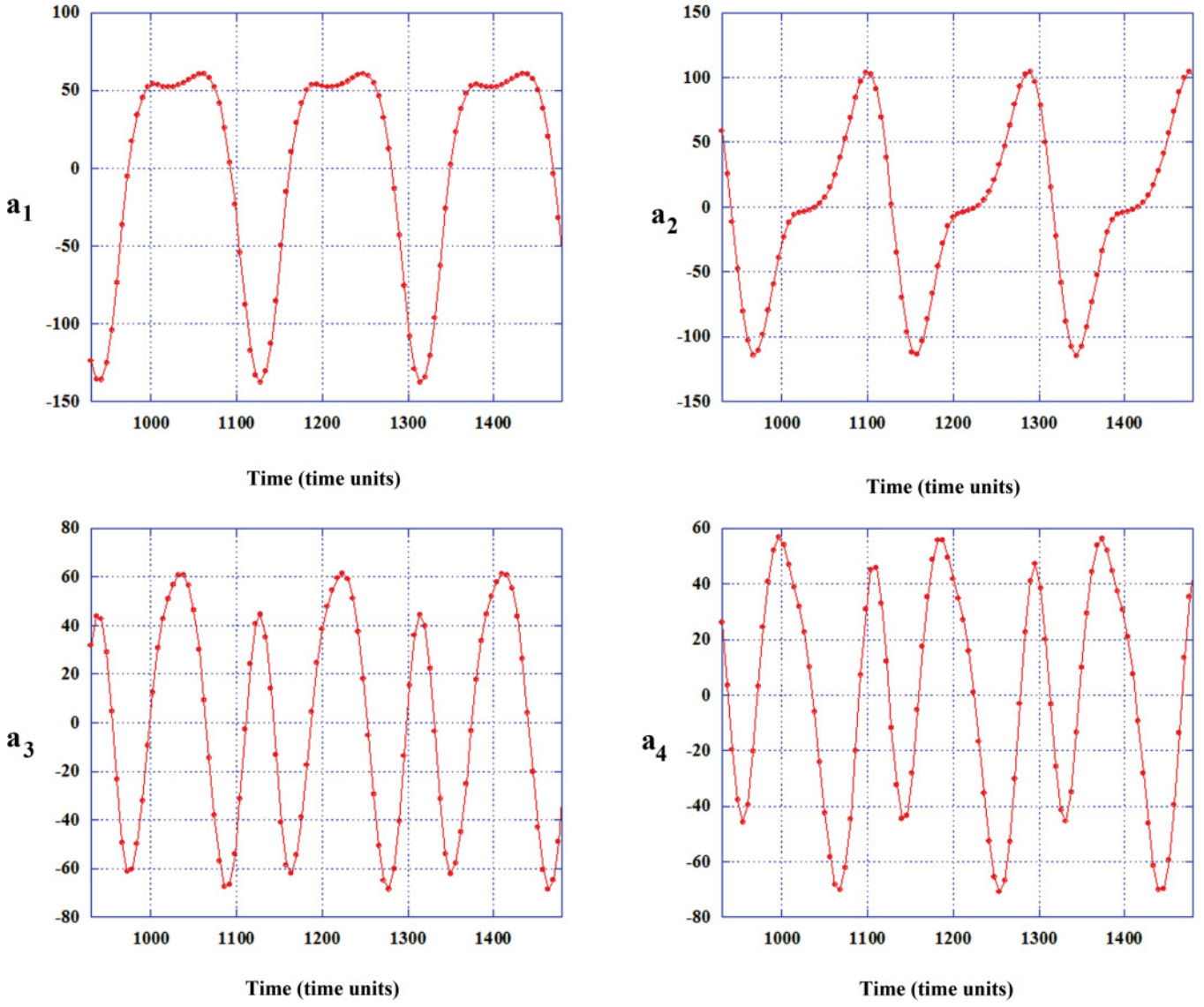


FIG. 8. (Color online) The projections of the $v$-pattern onto the eigenvectors, $a_i$ (for $t_1 = 930$, $t_2 = 1480$, $\Delta t = 6$).

the related eigenvectors. The left-hand eigenvectors, $U_j(x)$ are the dominant spatial time-averaged modes mentioned above, which constitute the vector basis for the PSTP. The projection of the latter on the basis yields time-dependent projection coefficients, $a_j\ (t)$. An $N$th-order best approximation to the vector $u(x,t_i)$ is obtained by

$$u\,(x,t_i) = \sum_{j=1}^{N} a_j\,(t_i)\;U_j\,(x). \tag{2}$$

Each eigenvector can subsequently be reconverted into a picture of the respective mode.

The SVD analysis was carried out for two complete periods, 240–618 time units; different $\Delta t$'s and different time spans (each including two complete periods) up to 9000 time units were used with no significant changes in both the eigenvalues and the eigenmodes. The eigenvalues for $v$ are shown in Fig. 6.

First, note that the values appear somewhat in pairs. Usually a pair of eigenvalues is considered to indicate a moving pattern. This movement can be inferred [27] from the two modes and the time evolution of the two projection amplitudes. In the case discussed here, the first two eigenvalues are above 500. Their corresponding vectors are the first two appearing in Fig. 7 and the temporal projection amplitudes are shown in Fig. 8. These projections are not as simple as those in Ref. [27]. The latter consist of two simple oscillations shifted by 90° in phase from each other. Figure 8 shows a somewhat different behavior. The two projections are not copies of each other and are not portraying simple oscillatory patterns. Therefore, they do not describe a simple movement of the structure. The combination of the two modes, $a_1(t)u_1 + a_2(t)u_2$, is depicted in Fig. 9 for the same times as in Fig. 1. It is seen that: i) Utilizing only the first two modes the result is already quite similar to the complete pattern (Fig. 1). This demonstrates the power of the SVD method. ii). No movement of the pattern, except for a possible outward one, is observed.

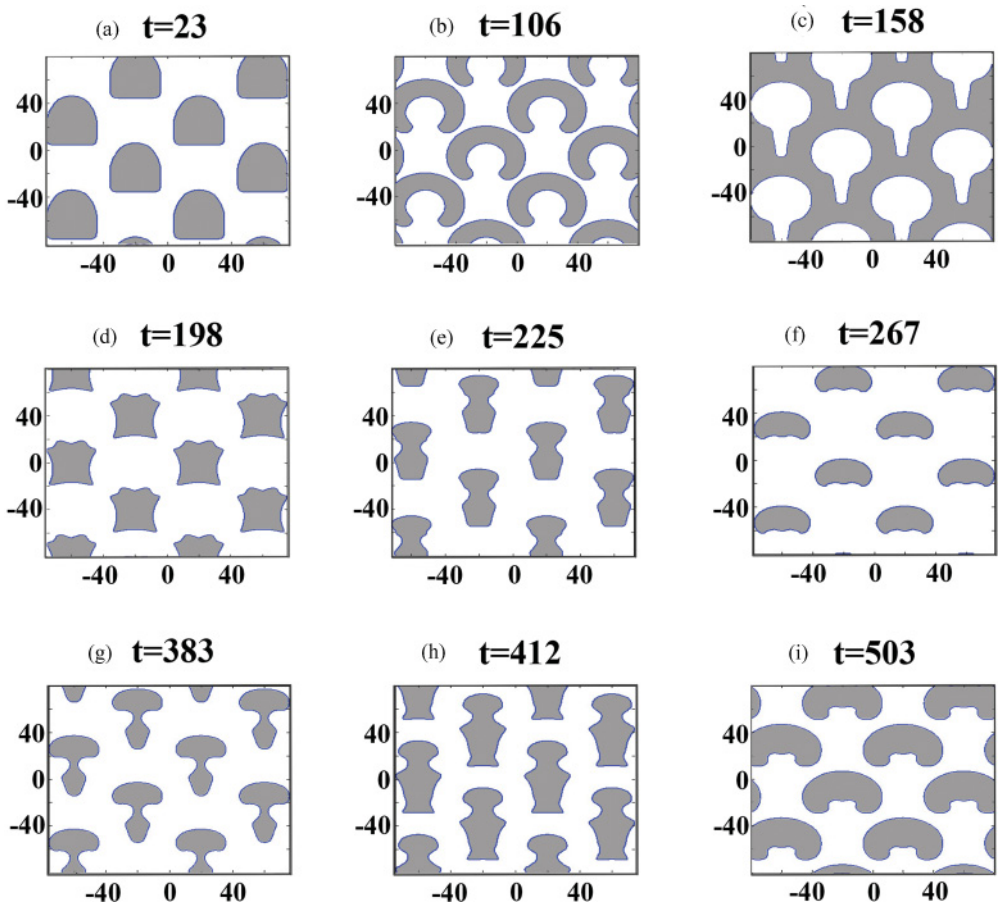


FIG. 9. (Color online) Reconstruction of $v$ with two modes. Gray areas: $v > 0.5$. Compare to Fig. 1.

Returning to the eigenmodes themselves (Fig. 7) they reveal the inner structure of the patterns. The first six modes are the important ones as they incorporate most of the energy as manifested by their eigenvalues. It is seen that the spiral pairs (A) are the most accentuated detail, appearing in all the first four modes. The final RPs (B) only appear in mode 6, presumably due to their short lifetime, while their predecessors (C) are already present in modes 1 and 3. This short lifetime should not be looked upon as lack of importance, since without these RPs no time-repeating patterns are possible.

## VI. CONCLUSION

Using the unidirectional method of creation, a pattern of spiral pairs, both time- and spatial-periodic, was shown to be a valid solution of the FitzHugh-Nagumo system. Its generation was explained by the encounter and partial annihilation of multiple spiral pairs, leaving behind a system of residual portions, which, like the phoenix, resurrect the former pattern. SVD methods were invoked to derive the most important modes of the waves. These were shown to be the spiral pairs and the residual portions. Susceptibility of the patterns to symmetry-breaking perturbations was demonstrated.

[1] J. L. Hammack, D. M. Henderson, and H. J. Segur, Fluid Mech. **532**, 1 (2005) and references therein.
[2] S. Schmitt and M. Lucke, Phys. Rev. A **44**, 4986 (1991).
[3] See e.g., M. D. Ezekowitz and J. A. Levine, JAMA **281**, 1830 (1999).
[4] A. C. Skanes, R. Mandapati, O. Berenfeld, J. M. Davidenko, and J. Jalife, Circulation **98**, 1236 (1998).
[5] J. Jaliffe, Cardiovas. Electrophysiol. **14**, 776 (2003).
[6] M. Yoshioka, Phys. Rev. Lett. **102**, 158102 (2009).
[7] A. Roxin, V. Hakim, and M. Brunel, J. Neurosci. **28**, 10734 (2008).
[8] J. Rinzel, J. Math. Biol. **5**, 363 (1978).
[9] S. P. Hastings, Quart. J. Math. **27**, 123 (1976).
[10] S. P. Hastings, SIAM J. Appl. Math. **42**, 247 (1982).
[11] T. Ivancevic, L. Jain, and J. Pattison, Nonlinear Dyn. **56**, 23 (2009).
[12] See e.g., J. D. Murray, in *Mathematical Biology*, 2nd ed. (Springer-Verlag, Berlin, 1993), pp. 161 ff., 350 ff.
[13] T. Tsujikawa, T. Nagai, M. Mimura, R. Kobayashi, and H. Ikeda, Jpn. J. Appl. Math. **6**, 341 (1989).
[14] M. Hoerning, A. Isomura, K. Agladze, and K. Yoshikawa, Phys. Rev. E **79**, 026218 (2009).

[15] B. Fiedler and R. M. Mantel, Documenta Math. **5**, 695 (2000).
[16] A. Rabinovitch, M. Gutman, Y. Biton, I. Aviram, and D. S. Rosenbaum, Phys. Rev. E **74**, 061904 (2006).
[17] Y. Biton, A. Rabinovitch, D. Braunstein, M. Friedman, and I. Aviram, Phys. Lett. A **375**, 2333 (2011).
[18] M. Friedman, I. E. Ovsyshcher, I. Fleidervish, E. Crystal, and A. Rabinovitch, Phys. Rev. E **70**, 041903 (2004).
[19] See Supplemental Material at http://link.aps.org/supplemental/10.1103/PhysRevE.85.036217 for videos.
[20] I. S. Aranson and L. Kramer, Rev. Mod. Phys. **74**, 99 (2002).
[21] I. S. Aranson and L. M. Pismen, Phys. Rev. Lett. **84**, 634 (2000) and references therein.
[22] I. S. Aranson, L. Aranson, L. Kramer, and A. Weber, Phys. Rev. A **46**, R2992 (1992).
[23] A. Rabinovitch, Y. Biton, M. Gutman, and I. Aviram, Comp. Biol. Med. **39**, 405 (2009).
[24] K. Karhunen, Am. Acad. Scientiarum Fennicae Series A **37**, 3 (1946).
[25] M. Loeve, *Probability Theory* (Van Nostrand, Toronto, 1955).
[26] L. Sirovich, Q. Appl. Math. **45**, 561 (1987).
[27] S. Sanghi and N. Hasan, Asia-Pacific J. Chem. Eng. **6**, 120 (2011).